

DiEC: Diffusion Embedded Clustering

Haidong Hu¹, Jin Zhou^{2*}

¹University of Jinan

²Shandong Women’s University

227088255@qq.com, zhoujin@sdwu.edu.cn

Abstract

Deep clustering critically depends on representations that expose clear cluster structure, yet most prior methods learn a single embedding with an autoencoder or a self-supervised encoder and treat it as the primary representation for clustering. In contrast, a pretrained diffusion model induces a rich representation trajectory over network layers and noise timesteps, along which clusterability varies substantially. We propose Diffusion Embedded Clustering (DiEC), an unsupervised clustering framework that exploits this trajectory by directly leveraging intermediate activations of a pretrained diffusion U-Net. DiEC formulates representation selection over $layer \times timestep$ and adopts a practical two-stage procedure: it uses the U-Net bottleneck as the Clustering Middle Layer (CML; l^*) and identifies the Clustering-Optimal Timestep (COT; t^*) via an efficient subset-based, noise-averaged search. Conditioning on (l^*, t^*) , DiEC learns clustering embeddings through a lightweight residual mapping, optimized with a DEC-style KL self-training objective and structural regularization, while a parallel random-timestep denoising-consistency loss stabilizes training and preserves diffusion behavior. Experiments on standard benchmarks demonstrate that DiEC achieves strong clustering performance and reveal the importance of selecting diffusion representations for clustering.

1 Introduction

Clustering is a fundamental task in unsupervised learning, aiming to uncover latent class structure from unlabeled data, and has been widely used in applications such as image understanding [Van Gansbeke *et al.*, 2020], anomaly detection [Pang *et al.*, 2021], and large-scale retrieval [Johnson *et al.*, 2019]. However, modern data are often high-dimensional, nonlinear, and corrupted by noise, making clustering increasingly dependent on high-quality and robust feature representations [Zhou *et al.*, 2024a]. Traditional approaches typically

rely on shallow features or simple distance metrics, and thus struggle to capture deep semantic structure in complex data [Ben-David, 2018]. Recent studies have therefore introduced deep models into clustering by jointly optimizing representation learning and clustering objectives, improving performance in challenging settings [Zhou *et al.*, 2024a]. This line of research is commonly referred to as deep clustering and has been validated by representative methods such as those of [Ren *et al.*, 2024] and [Wei *et al.*, 2024].

Existing deep clustering methods have made progress in high-dimensional, nonlinear, and noisy settings largely because deep networks can learn more semantically meaningful representations, thereby improving cluster separability in the resulting embedding space [Zhou *et al.*, 2024b]. Accordingly, much of the literature centers on how to obtain clustering-friendly representations [Zhou *et al.*, 2024b]. Existing approaches have broadly evolved along two complementary lines: (i) generative encoders, represented by autoencoders, variational autoencoders, and GANs, which learn low-dimensional embeddings via reconstruction or generation objectives [Xie *et al.*, 2016; Jiang *et al.*, 2017; Mukherjee *et al.*, 2019]; and (ii) discriminative self-supervised learning, represented by contrastive learning, which enforces consistency constraints to learn discriminative representations [Van Gansbeke *et al.*, 2020; Caron *et al.*, 2020]. Despite the different training signals, both families typically share a common modeling assumption: the feature extractor naturally yields a single, most clustering-discriminative primary representation, on top of which cluster assignment and structure refinement are performed [Xie *et al.*, 2016; Zhou *et al.*, 2024b].

We observe that the clusterability of internal representations in diffusion denoising networks is not random; instead, it varies systematically with both the noise scale and the network hierarchy. Along the noise scale, clustering performance often follows a unimodal trend, improving at moderate noise levels and degrading at high noise levels. Along the network hierarchy, clusterability typically peaks in the early upsampling stages immediately after the bottleneck, where representations remain stable while becoming increasingly separable. Moreover, across datasets, bottleneck activations are easy to extract and provide a reliably strong clustering signal, though they are not necessarily optimal. In contrast, post-bottleneck representations often require higher extrac-

*Corresponding author.

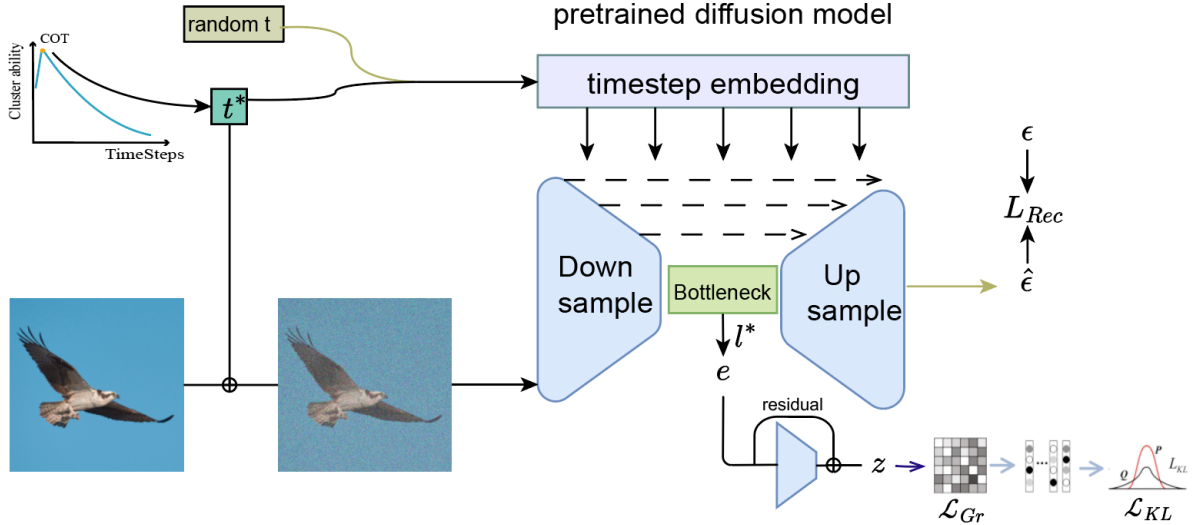


Figure 1: **Overview of DiEC (Diffusion Embedded Clustering)**. Given an input image x_0 , we inject noise using both a random timestep t_{rand} and a fixed clustering-optimal timestep (COT). The random-timestep branch preserves generative consistency via standard denoising, while the fixed-timestep branch extracts the Clustering Middle Layer (CML) for clustering-aware optimization. We apply residual decoupling on CML and jointly optimize a graph regularizer and a KL-based clustering objective to achieve more stable and discriminative clustering representations.

tion cost with only marginal gains, which motivates us to focus on bottleneck features in our design.

Motivated by the above patterns, we propose **Diffusion Embedded Clustering (DiEC)**, a framework that performs unsupervised clustering by leveraging internal representations from the denoising network of a pretrained diffusion model. DiEC treats internal activations generated under different noise conditions and network hierarchies as a searchable representation trajectory, and builds the clustering pipeline on top of it: we select the bottleneck layer as the **Clustering Middle Layer (CML)** and efficiently identify the **Clustering-Optimal Timestep (COT)** via a fast scan on a data subset. We then introduce clustering optimization in this representation space, sharpening assignments with a KL-divergence-based clustering loss, preserving local structure through adaptive graph embedding, and alleviating potential conflicts between denoising and clustering objectives via residual feature decoupling, which strengthens cluster structure and improves clustering performance. Experiments and systematic ablations show that DiEC outperforms existing deep clustering methods on multiple benchmark datasets. Our contributions are as follows:

- We propose **DiEC**, the first framework to perform clustering by exploiting **internal representations** of pretrained diffusion models.
- We introduce **representation-trajectory perspective** and show that clusterability varies systematically over the $\text{timestep} \times \text{layer}$ space; based on this insight, we identify a more clustering-friendly layer location and develop an efficient procedure to quickly localize the clustering-optimal timestep.

- We design a clustering-aware optimization that combines residual feature decoupling with a KL-based clustering loss and graph-embedding regularization, improving training stability and mitigating conflicts between denoising and clustering objectives.
- Extensive benchmark results demonstrate that DiEC achieves clear improvements on clustering metrics over deep clustering methods built on traditional generative representations such as AE/VAE/GAN.

2 Related Work

Clustering in Learned Embedding Spaces. Most prior work follows a two-stage paradigm: it first learns a feature extractor $f(x) \rightarrow z$ and then performs cluster-assignment optimization in the embedding space z , where autoencoders and other generative models mainly serve as representation learners. An early representative method is DEC [Xie *et al.*, 2016], which builds on a pretrained autoencoder and learns soft cluster assignments in a low-dimensional embedding space by matching them to an auxiliary target distribution. While DEC can learn clustering-oriented representations effectively, its performance is often sensitive to initialization, and training may suffer from degenerate solutions.

Building on variational autoencoders (VAEs), VaDE [Jiang *et al.*, 2017] explicitly injects a clustering structure into the latent space and jointly learns the generative model, latent representations, and cluster assignments under a variational inference framework. However, VaDE typically relies on a well-initialized pretrained stage, and can be sensitive to modeling assumptions and hyperparameters in high-dimensional or complex data regimes.

Within the GAN framework, ClusterGAN [Mukherjee *et al.*, 2019] introduces an additional inverse mapping $E(\cdot)$ alongside the generator, so that the inferred code $z = E(x)$ aligns with the latent prior of the generator. Training is guided by a closed-loop *latent regression* constraint, $z \rightarrow x = G(z) \rightarrow \hat{z} = E(x)$, encouraging z to serve as a faithful generative-space representation from which cluster indicators can be read out (e.g., via discrete latent components) or obtained by clustering in z . However, such methods rely on adversarial min-max optimization and often face challenges in stability and scalability. In contrast, recent work has increasingly explored diffusion models as an alternative paradigm for generative modeling and representation learning [Ho *et al.*, 2020; Song and Ermon, 2021].

Moreover, generic deep neural networks (DNNs), e.g., CNNs, are also widely used as feature extractors. These methods typically learn representations via contrastive learning or consistency regularization, and then optimize cluster assignments in the learned embedding space, with representative examples including Contrastive Clustering (CC) [Li *et al.*, 2021] and SCAN [Van Gansbeke *et al.*, 2020]. Since this paper focuses on generative representation learning paradigms, we primarily compare clustering methods built on autoencoders and generative models; approaches based on contrastive learning or consistency constraints are not treated as our main comparison targets.

Diffusion Models as Feature Extractors. In recent years, a growing body of work has explored using diffusion models as feature extractors to provide discriminative representations for downstream vision tasks; for a systematic overview, we refer to [Fuest *et al.*, 2024] for a comprehensive survey. Existing studies that leverage diffusion models for representation extraction can be broadly categorized into two groups.

The first line of work treats diffusion models as a *representation source*: without substantially modifying the model architecture, it directly reads intermediate features from the denoising network at selected timesteps or layers and uses them for downstream tasks. These methods typically use a pre-trained diffusion model as a frozen or lightly adapted backbone, and focus on characterizing the discriminative power of features across timesteps and hierarchies. Representative examples include DDAE [Xiang *et al.*, 2023], DIFT [Tang *et al.*, 2023], and Diffusion Hyperfeatures [Luo *et al.*, 2023].

A second line of work redesigns diffusion models as *explicit* representation learners by introducing structured latent variables, bottlenecks, or reconstruction constraints, so that diffusion training directly optimizes a semantically meaningful representation space instead of merely reading intermediate activations. Representative methods include Diffusion Autoencoders [Preechakul *et al.*, 2022], InfoDiffusion [Wang *et al.*, 2023], and SODA [Hudson *et al.*, 2024], which leverage the diffusion process itself to learn stable and decodable representations.

However, these approaches typically evaluate representation quality using discriminative criteria such as linear-probe classification, and do not explicitly address the challenges specific to fully unsupervised clustering.

Diffusion for Clustering. Research on introducing diffusion models into fully unsupervised clustering remains limited. CLUDI [Uziel *et al.*, 2025] trains a conditional diffusion model on top of frozen pretrained ViT features, samples *assignment embeddings*, and improves stability by averaging multiple samples; its core training signal is a teacher-student consistency alignment, while inference relies on multi-step reverse diffusion sampling and can be time-consuming. ClusterDDPM [Yan *et al.*, 2025] instead uses conditional diffusion to model cluster-related generative factors, making it closer to conditional generative modeling. In contrast, DiEC asks whether the *denoising network itself* can serve as a feature extractor for clustering, rather than relying on a frozen external representation or using diffusion mainly for assignment sampling and consistency modeling.

3 Background

Diffusion models. Compared with traditional generative models such as VAEs and GANs, diffusion models often offer a better trade-off between sample fidelity and training stability, and have demonstrated strong performance in image synthesis, text-to-image generation, image editing, super-resolution, and other conditional generation tasks [Dhariwal and Nichol, 2021; Nichol *et al.*, 2022; Saharia *et al.*, 2021; Saharia *et al.*, 2022]. These advances have established diffusion models as a leading paradigm for high-fidelity generative modeling.

The core idea of diffusion models is to formulate generation as iterative denoising: a forward process gradually corrupts data with Gaussian noise, and a learned reverse-time process progressively removes noise to generate samples from the data distribution.

In DDPM [Ho *et al.*, 2020], the forward diffusion process is defined as a Markov chain that gradually corrupts a data sample $x_0 \sim q_{\text{data}}(x)$:

$$q(x_t | x_{t-1}) = \mathcal{N}(x_t; \sqrt{1 - \beta_t} x_{t-1}, \beta_t \mathbf{I}), \quad (1)$$

where $\{\beta_t\}_{t=1}^T$ is a predefined noise schedule and $t \in \{1, \dots, T\}$ denotes the diffusion timestep. Let $\alpha_t = 1 - \beta_t$ and $\bar{\alpha}_t = \prod_{i=1}^t \alpha_i$. Then, the marginal distribution of x_t admits a closed-form expression

$$x_t = \sqrt{\bar{\alpha}_t} x_0 + \sqrt{1 - \bar{\alpha}_t} \epsilon, \quad \epsilon \sim \mathcal{N}(0, \mathbf{I}), \quad (2)$$

which shows that the noise level of x_t is fully governed by the timestep t .

The reverse-time process is parameterized as a Gaussian transition

$$p_{\theta}(x_{t-1} | x_t) = \mathcal{N}(x_{t-1}; \mu_{\theta}(x_t, t), \sigma_t^2 \mathbf{I}), \quad (3)$$

where the mean is expressed via a noise-prediction network ϵ_{θ} as

$$\mu_{\theta}(x_t, t) = \frac{1}{\sqrt{\alpha_t}} \left(x_t - \frac{\beta_t}{\sqrt{1 - \bar{\alpha}_t}} \epsilon_{\theta}(x_t, t) \right), \quad (4)$$

and the variance is fixed to the posterior value

$$\sigma_t^2 = \tilde{\beta}_t = \frac{1 - \bar{\alpha}_{t-1}}{1 - \bar{\alpha}_t} \beta_t. \quad (5)$$

In practice, the neural network $\epsilon_\theta(x_t, t)$ predicts the forward-process noise ϵ and is trained with a simple mean-squared error objective:

$$\mathcal{L}(\theta) = \mathbb{E}_{t, x_0, \epsilon} \left[\|\epsilon - \epsilon_\theta(x_t, t)\|_2^2 \right]. \quad (6)$$

This objective can be interpreted as a simplified variational bound on the data likelihood. At sampling time, starting from $x_T \sim \mathcal{N}(0, \mathbf{I})$, the reverse transition $p_\theta(x_{t-1} | x_t)$ is applied iteratively to progressively denoise samples and generate data.

It is worth noting that DDPMs are formulated with discrete timesteps, while subsequent work has also developed continuous-time variants and provided a unified view of diffusion processes from the perspective of stochastic differential equations (SDEs) [Song and Ermon, 2021]. The noise-prediction network $\epsilon_\theta(x_t, t)$ is typically implemented with a U-Net architecture [Ronneberger *et al.*, 2015], and recent studies have explored using Vision Transformers (ViTs) as the denoising backbone [Dosovitskiy *et al.*, 2021; Peebles and Xie, 2023]. In this paper, we adopt the discrete-time DDPM formulation and a U-Net noise predictor to stay consistent with our subsequent analysis on timestep selection.

DEC-style Clustering Objective. Deep Embedded Clustering (DEC) performs unsupervised clustering by jointly learning sample embeddings and cluster centroids [Xie *et al.*, 2016]. Given an embedding z_i and centroids $\{\mu_k\}_{k=1}^K$, DEC defines the soft assignment via a Student’s t -distribution kernel:

$$q_{ik} = \frac{(1 + \|z_i - \mu_k\|^2/\alpha)^{-\frac{\alpha+1}{2}}}{\sum_{k'} (1 + \|z_i - \mu_{k'}\|^2/\alpha)^{-\frac{\alpha+1}{2}}}. \quad (7)$$

To emphasize high-confidence assignments and mitigate cluster-size imbalance, DEC constructs a target distribution $P = [p_{ik}]$ from $Q = [q_{ik}]$:

$$p_{ik} = \frac{q_{ik}^2 / \sum_i q_{ik}}{\sum_{k'} (q_{ik'}^2 / \sum_i q_{ik'})}. \quad (8)$$

DEC then minimizes the KL divergence $\text{KL}(P||Q) = \sum_i \sum_k p_{ik} \log \frac{p_{ik}}{q_{ik}}$ for self-training, progressively sharpening the soft assignments and improving clustering consistency.

4 Diffusion Embedded Clustering

Let $x_{t,i}$ denote the noisy version of the i -th sample at diffusion timestep t , and $x_{0,i}$ its corresponding clean input. Given an unlabeled dataset $\mathcal{D} = \{x_{0,i}\}_{i=1}^N$ and the number of clusters K , DiEC leverages intermediate activations of a pre-trained diffusion model to learn clusterable representations and infer a cluster assignment $\hat{y}_i \in \{1, \dots, K\}$ for each sample.

DiEC first identifies a clustering-friendly location on the diffusion representation trajectory, specified by a *layer-timestep* pair (l^*, t^*) . Conditioning on (l^*, t^*) , it extracts the corresponding features and optimizes a DEC-style clustering objective together with a structural regularizer, yielding stable and well-separated embeddings. Figure 1 provides an overview of the framework, and we present implementation details in the following subsections.

4.1 Locating Clustering-Friendly Diffusion Representations

We view the internal activations produced by a pretrained diffusion denoising network at different noise timesteps t and network layers l as a *representation trajectory*. Representations at different locations (t, l) can exhibit markedly different clustering quality, which we measure using an unsupervised scoring function $S(\cdot)$. Ideally, one would jointly select the optimal representation in the two-dimensional (t, l) space; however, a brute-force search requires $\mathcal{O}(|T||L|)$ evaluations (each involving feature extraction and clustering), which is prohibitively expensive. Empirically, we further observe that, for most datasets, the optimal layer remains stable over a wide range of timesteps, while the optimal timestep varies only mildly across nearby layers (see Sec. 5). Motivated by this weak-coupling behavior, we approximately decompose the 2D selection into two stages: we first fix the middle-layer readout location for clustering (CML), denoted by l^* , and then search for the clustering-optimal timestep (COT) on that layer, denoted by t^* .

Clustering Middle Layer (CML). In the denoising network of a pretrained diffusion model, features at different layers capture semantic abstractions at different granularity: shallow layers tend to encode local textures and noise details, whereas deeper layers are closer to the noise-prediction objective near the output. We define the bottleneck layer between the U-Net downsampling and upsampling paths as the *Clustering Middle Layer (CML)*, denoted by l^* . For a sample $x_{0,i}$, given its noisy observation $x_{t,i}$ at timestep t , we read the activation at layer l^* and flatten it to obtain

$$e_i(t) = h_\theta^{l^*}(x_{t,i}, t). \quad (9)$$

In our experiments, the performance differences induced by layer selection are generally small (see Sec. 5). Therefore, DiEC does not treat layer search as a primary optimization target; instead, we fix CML to the U-Net bottleneck to balance computational efficiency and reproducibility. We accordingly focus on localizing the clustering-optimal timestep (COT) and the subsequent clustering-aware optimization.

Clustering-Optimal Timestep (COT). Under the condition of a fixed layer l^* , we define an unsupervised clustering-quality score $S(t)$ to measure clusterability at timestep t . We then define the clustering-optimal timestep as

$$t^* = \arg \max_{t \in \mathcal{T}} S(t), \quad (10)$$

where \mathcal{T} is the candidate set of timesteps. We refer to t^* as the *Clustering-Optimal Timestep (COT)*.

To reduce the randomness introduced by diffusion noising, we optionally evaluate $S(t)$ by repeating the sampling at the same timestep t for a few trials and averaging the scores. We describe in the next subsection how to efficiently localize t^* while maintaining reliable evaluation, via the proposed Optimal Timestep Search (OTS).

Optimal Timestep Search (OTS). We seek to solve $t^* = \arg \max_{t \in \mathcal{T}} S(t)$, where $S(t)$ is an unsupervised score that measures the clusterability of $\{e_i(t)\}$. A naive strategy evaluates $S(t)$ for every $t \in \mathcal{T}$, which incurs $\mathcal{O}(|\mathcal{T}|)$ complexity, grows linearly with $|\mathcal{T}|$, and requires feature extraction and one clustering run per evaluation. To this end, we

propose *Optimal Timestep Search (OTS)*, which combines subset-based approximation and noise averaging to obtain a controlled-variance estimate of $S(t)$, and further leverages an approximate unimodality assumption to localize t^* with only logarithmically many evaluations.

Subset-based approximation and noise-averaged scoring. Let the full unlabeled dataset be $\mathcal{D} = \{x_{0,i}\}_{i=1}^N$. OTS samples a subset $\mathcal{D}_s \subset \mathcal{D}$ with $|\mathcal{D}_s| = m$. For each $x_{0,i} \in \mathcal{D}_s$, at a given timestep t we repeat R forward noising trials by drawing $\xi_i^{(r)} \sim \mathcal{N}(0, \mathbf{I})$ and constructing

$$x_{t,i}^{(r)} = \sqrt{\alpha_t} x_{0,i} + \sqrt{1 - \alpha_t} \xi_i^{(r)}, \quad r = 1, \dots, R, \quad (11)$$

together with the corresponding intermediate embeddings

$$e_i^{(r)}(t) = h_\theta^*(x_{t,i}^{(r)}, t). \quad (12)$$

We then reduce stochasticity via noise averaging:

$$\bar{e}_i(t) = \frac{1}{R} \sum_{r=1}^R e_i^{(r)}(t). \quad (13)$$

Finally, we run a lightweight clustering (e.g., k -means) on $\{\bar{e}_i(t)\}_{x_{0,i} \in \mathcal{D}_s}$ and compute the Calinski–Harabasz index (CHI), yielding a subset- and noise-averaged estimate

$$\widehat{\text{CHI}}_{m,R}(t) = \text{CHI}(\{\bar{e}_i(t)\}_{x_{0,i} \in \mathcal{D}_s}). \quad (14)$$

Lemma 1 (Consistency of noise averaging). For a fixed sample x_i and timestep t , if $\mathbb{E} \left[\left\| e_i^{(r)}(t) \right\| \right] < \infty$, then as $R \rightarrow \infty$,

$$\bar{e}_i(t) = \frac{1}{R} \sum_{r=1}^R e_i^{(r)}(t) \xrightarrow{\text{a.s.}} \mathbb{E}_\xi[e(x_i, \xi, t)]. \quad (15)$$

Proof sketch. Since $\{e_i^{(r)}(t)\}_{r=1}^R$ are i.i.d. with respect to the noise ξ , the almost sure convergence follows from the strong law of large numbers.

Lemma 2 (Convergence of the subset statistic, conditional on stable partition). Let $z_i(t) = \mathbb{E}_\xi[e(x_i, \xi, t)]$. If at timestep t the optimal k -means partition remains stable under local perturbations (e.g., the optimum is unique with a positive margin), then as $m \rightarrow \infty$ and $R \rightarrow \infty$,

$$\widehat{\text{CHI}}_{m,R}(t) \xrightarrow{\text{a.s.}} \text{CHI}(\{z_i(t)\}_{i=1}^N). \quad (16)$$

That is, the OTS score estimator concentrates as both the subset size and the noise averaging increase.

Proof sketch. By Lemma 1, $\bar{e}_i(t)$ converges to $z_i(t)$. Under the partition-stability condition, CHI is determined by sample statistics such as cluster means and within-/between-cluster scatter, which satisfy the law of large numbers under sample averaging; the desired convergence of $\widehat{\text{CHI}}_{m,R}(t)$ then follows via continuity of the mapping from these statistics to CHI.

4.2 Clustering-Aware Optimization

In this section, conditioned on t^* , we extract intermediate embeddings e_i from the U-Net CML and obtain clustering representations z_i via a lightweight residual mapping. We jointly optimize a DEC-style KL self-training objective and a graph

regularizer on z_i to strengthen cluster structure, while introducing a standard denoising loss at a random timestep t_{rand} to maintain diffusion consistency and stabilize the representations.

Residual-decoupled embedding. After determining t^* and l^* , for each sample x_i we construct its noisy input $x_{t^*,i}$ at timestep t^* and extract the bottleneck activation from the U-Net:

$$e_i = h_\theta^{l^*}(x_{t^*,i}, t^*). \quad (17)$$

We introduce a lightweight residual mapping $g_\phi(\cdot)$ and obtain the final clustering representation as

$$z_i = e_i + g_\phi(e_i). \quad (18)$$

Here, g_ϕ is a small MLP that captures clustering-relevant factors from e_i . Empirically, this mapping improves the discriminability between clusters while maintaining the stability of the underlying diffusion features.

Intuitively, clustering and diffusion denoising optimize different objectives and may impose conflicting requirements on representations. The residual design helps preserve the local structure of the original features, while allowing the clustering loss to adjust the representation toward being more clusterable, thereby mitigating interference from the denoising objective.

Clustering objective. Following the DEC framework introduced in Sec. 3, we adopt a KL-divergence-based self-training objective on the learned representations $\{z_i\}$. Specifically, for each sample $x_{0,i}$, we apply forward noising at the fixed clustering-optimal timestep t^* to obtain $x_{t^*,i}$ and extract its intermediate representation via the CML. To reduce the stochasticity induced by diffusion noise, we draw M independent noise realizations at t^* , obtain the corresponding representations $\{z_i^{(m)}\}_{m=1}^M$ through the residual module, and average them to form a stabilized feature

$$z_i = \frac{1}{M} \sum_{m=1}^M z_i^{(m)}. \quad (19)$$

Given $\{z_i\}$, we initialize cluster centroids using k -means and follow DEC to compute the soft assignments Q and the target distribution P . We then minimize the KL divergence $\text{KL}(P||Q)$ to progressively sharpen high-confidence assignments, and denote this objective as \mathcal{L}_{KL} .

Adaptive graph regularization. Optimizing only \mathcal{L}_{KL} may be insufficient to preserve local geometric consistency in the embedding space. We therefore introduce an adaptive graph regularizer. Concretely, given the current representations, we construct a k -NN neighborhood NB_i for each sample and learn a row-normalized affinity matrix $\mathbf{S} = [s_{ij}]$. We impose a local-consistency constraint on the soft assignments Q :

$$\begin{aligned} \mathcal{L}_{\text{Gr}} &= \sum_{i=1}^N \sum_{j \in \text{NB}_i} \sum_{k=1}^K s_{ij} (q_{ik} - q_{jk})^2, \\ \text{s.t.} \quad &\sum_{j \in \text{NB}_i} s_{ij} = 1, \quad s_{ij} \in [0, 1]. \end{aligned} \quad (20)$$

and add an entropy regularizer to avoid degenerate weights:

$$\mathcal{L}_{\text{En}} = \sum_{i=1}^N \sum_{j \in \text{NB}_i} s_{ij} \log s_{ij}. \quad (21)$$

Joint training with diffusion consistency. The clustering branch imposes constraints only at the fixed optimal timestep t^* . If we directly update the shared denoising network parameters using this signal alone, the denoising capability at other timesteps may degrade, undermining the overall stability of diffusion representations. To prevent this, we introduce an additional consistency branch at random timesteps. At each iteration, we sample $t_{\text{rand}} \sim \mathcal{U}(\{1, \dots, T\})$, apply the standard forward noising to obtain $x_{t_{\text{rand}}, i}$, and train the network with the same noise-prediction MSE objective as in the diffusion background, thereby preserving the generative consistency of the pretrained diffusion model. Concretely, the diffusion-consistency loss is

$$\mathcal{L}_{\text{Re}} = \mathbb{E}_{t_{\text{rand}}, \epsilon} \left[\frac{1}{N} \sum_{i=1}^N \|\epsilon - \epsilon_{\theta}(x_{t_{\text{rand}}, i}, t_{\text{rand}})\|_2^2 \right]. \quad (22)$$

4.3 Loss Function

We optimize the diffusion U-Net (together with the residual module) end-to-end with a weighted combination of objectives. The overall training objective is

$$\mathcal{L} = \alpha \mathcal{L}_{\text{KL}} + \beta \mathcal{L}_{\text{Gr}} + \gamma \mathcal{L}_{\text{En}} + \mathcal{L}_{\text{Re}}, \quad (23)$$

where \mathcal{L}_{KL} is the DEC-style clustering loss, \mathcal{L}_{Gr} and \mathcal{L}_{En} are the adaptive graph regularizer and the entropy regularizer (see Sec. 4.2), and \mathcal{L}_{Re} is the diffusion-consistency denoising reconstruction loss at random timesteps (see Sec. 4.2). The scalars α , β , and γ are weighting hyperparameters that balance the relative contributions of the loss terms.

We fix the weight of \mathcal{L}_{Re} to 1 to keep the loss scale consistent with the pretraining objective and to avoid the clustering signal at the fixed t^* dominating the shared-parameter updates. In practice, γ mainly prevents degenerate graph weights and is not sensitive to its exact value, so a small constant suffices. The complete training procedure and the alternating updates are summarized in Algorithm 1.

5 Experiment

Datasets. We evaluate DiEC on four widely used benchmarks for unsupervised clustering: MNIST, USPS, Fashion-MNIST, and CIFAR-10. MNIST and Fashion-MNIST each contain 70,000 grayscale images of resolution 28×28 . USPS contains 9,298 grayscale handwritten-digit images with an original resolution of 16×16 . CIFAR-10 consists of 60,000 color images of resolution 32×32 . All datasets have 10 ground-truth classes. In our clustering setup, we treat all samples as unlabeled during training and set K to the true number of classes only for evaluation when computing clustering metrics. To match the diffusion model input, all images are normalized as a preprocessing step. The dataset statistics are reported in Table 1.

Dataset	Samples	Resolution	Classes
MNIST	70,000	28×28	10
USPS	9,298	16×16	10
Fashion-MNIST	70,000	28×28	10
CIFAR-10	60,000	32×32	10

Table 1: Datasets used in our experiments.

Method	MNIST	USPS	Fashion-MNIST	CIFAR-10
DEC	84.3	61.9	51.8	30.1
IDEC	88.1	76.1	–	–
DCEC	89.0	79.0	60.0	–
VaDE	94.4	56.6	62.9	26.7
ClusterGAN	95.0	–	63.0	28.1
DAC	97.8	–	–	52.2
DECRA	96.4	95.1	96.3	–
GammM-VAE	95.2	–	70.8	–
ClusterDDPM	97.7	–	70.5	30.5
DiEC (Ours)	99.5	98.2	80.1	60.1

Table 2: Clustering accuracy (ACC, %) on four benchmarks. ACC is computed after optimal label matching (Hungarian algorithm). Full metrics (ACC/NMI/ARI) will be reported in v2.

Evaluation metrics. We evaluate clustering performance using three standard metrics: clustering accuracy (ACC), normalized mutual information (NMI), and adjusted Rand index (ARI). These metrics quantify the agreement between predicted cluster assignments and ground-truth labels from complementary perspectives, including optimal label matching, information-theoretic consistency, and partition similarity with chance correction. Higher values indicate better clustering quality.

Results. Table 2 summarizes clustering accuracy (ACC) on MNIST, USPS, Fashion-MNIST, and CIFAR-10. Overall, **DiEC** achieves the best performance on all four benchmarks, demonstrating the effectiveness of exploiting pretrained diffusion internal representations for unsupervised clustering. In particular, DiEC yields strong gains over classical generative clustering baselines on MNIST/USPS and remains robust on the more challenging Fashion-MNIST and CIFAR-10, highlighting the benefit of the proposed representation selection (**CML+COT**) and the joint optimization with diffusion consistency.

6 Conclusion

We presented **DiEC (Diffusion Embedded Clustering)**, a diffusion-based deep clustering framework that performs unsupervised clustering by directly exploiting internal representations of a pretrained diffusion U-Net. DiEC views diffusion activations across *layer* \times *timestep* as a representation trajectory and identifies a clustering-friendly location by fixing the bottleneck layer (**CML**) and efficiently localizing the clustering-optimal timestep (**COT**) via **OTS**. Conditioning on (l^*, t^*) , we jointly optimize a DEC-style KL self-training objective together with adaptive graph and entropy regularization, while introducing a random-timestep

denoising-consistency branch to preserve diffusion stability. Experiments on four standard benchmarks demonstrate that DiEC achieves competitive clustering accuracy and validates the importance of selecting appropriate diffusion representations for clustering.

References

- [Ben-David, 2018] Shai Ben-David. Clustering — what both theoreticians and practitioners are doing wrong. In *Proceedings of the AAAI Conference on Artificial Intelligence*, volume 32, 2018.
- [Caron *et al.*, 2020] Mathilde Caron, Ishan Misra, Julien Mairal, Priya Goyal, Piotr Bojanowski, and Armand Joulin. Unsupervised learning of visual features by contrasting cluster assignments. *CoRR*, abs/2006.09882, 2020.
- [Dhariwal and Nichol, 2021] Prafulla Dhariwal and Alexander Quinn Nichol. Diffusion models beat GANs on image synthesis. In *Advances in Neural Information Processing Systems 34 (NeurIPS 2021)*, pages 8780–8794, 2021.
- [Dosovitskiy *et al.*, 2021] Alexey Dosovitskiy, Lucas Beyer, Alexander Kolesnikov, Dirk Weissenborn, Xiaohua Zhai, Thomas Unterthiner, Mostafa Dehghani, Matthias Minderer, Georg Heigold, Sylvain Gelly, Jakob Uszkoreit, and Neil Houlsby. An image is worth 16x16 words: Transformers for image recognition at scale. In *International Conference on Learning Representations (ICLR)*, 2021.
- [Fuest *et al.*, 2024] Michael Fuest, Pingchuan Ma, Ming Gui, Johannes Schusterbauer, Vincent Tao Hu, and Björn Ommer. Diffusion models and representation learning: A survey, 2024.
- [Ho *et al.*, 2020] Jonathan Ho, Ajay Jain, and Pieter Abbeel. Denoising diffusion probabilistic models. In *Advances in Neural Information Processing Systems (NeurIPS)*, 2020.
- [Hudson *et al.*, 2024] Drew A. Hudson, Daniel Zoran, Mateusz Malinowski, Andrew K. Lampinen, Andrew Jaegle, James L. McClelland, Loic Matthey, Felix Hill, and Alexander Lerchner. Soda: Bottleneck diffusion models for representation learning. In *Proceedings of the IEEE/CVF Conference on Computer Vision and Pattern Recognition (CVPR)*, pages 23115–23127, 2024.
- [Jiang *et al.*, 2017] Zhuxi Jiang, Yin Zheng, Huachun Tan, Bangsheng Tang, and Hanning Zhou. Variational deep embedding: An unsupervised and generative approach to clustering. In *Proceedings of the 26th International Joint Conference on Artificial Intelligence (IJCAI)*, pages 1965–1972, 2017.
- [Johnson *et al.*, 2019] Jeff Johnson, Matthijs Douze, and Hervé Jégou. Billion-scale similarity search with gpus. *IEEE Transactions on Big Data*, 7(3):535–547, 2019.
- [Li *et al.*, 2021] Yunfan Li, Peng Hu, Zitao Liu, Dezhong Peng, Joey Tianyi Zhou, and Xi Peng. Contrastive clustering. In *Proceedings of the AAAI Conference on Artificial Intelligence (AAAI)*, volume 35, pages 8547–8555, 2021.
- [Luo *et al.*, 2023] Grace Luo, Lisa Dunlap, Dong Huk Park, Aleksander Holynski, and Trevor Darrell. Diffusion hyperfeatures: Searching through time and space for semantic correspondence. In *Advances in Neural Information Processing Systems*, volume 36, 2023.
- [Mukherjee *et al.*, 2019] Sudipto Mukherjee, Himanshu Asnani, Eugene Lin, and Sreeram Kannan. Clustergan: Latent space clustering in generative adversarial networks. In *Proceedings of the AAAI Conference on Artificial Intelligence (AAAI)*, pages 4610–4617, 2019.
- [Nichol *et al.*, 2022] Alexander Quinn Nichol, Prafulla Dhariwal, Aditya Ramesh, Pranav Shyam, Pamela Mishkin, Bob McGrew, Ilya Sutskever, and Mark Chen. GLIDE: Towards photorealistic image generation and editing with text-guided diffusion models. In *Proceedings of the 39th International Conference on Machine Learning (ICML)*, volume 162 of *Proceedings of Machine Learning Research*, pages 16784–16804. PMLR, 2022.
- [Pang *et al.*, 2021] Guansong Pang, Chunhua Shen, Longbing Cao, and Anton van den Hengel. Deep learning for anomaly detection: A review. *ACM Computing Surveys*, 54(2), 2021.
- [Peebles and Xie, 2023] William Peebles and Saining Xie. Scalable diffusion models with transformers. In *Proceedings of the IEEE/CVF International Conference on Computer Vision (ICCV)*, 2023.
- [Preechakul *et al.*, 2022] Konpat Preechakul, Nattanat Chatthee, Suttisak Wizadwongsa, and Supasorn Suwajanakorn. Diffusion autoencoders: Toward a meaningful and decodable representation. In *Proceedings of the IEEE/CVF Conference on Computer Vision and Pattern Recognition (CVPR)*, pages 10609–10619, 2022.
- [Ren *et al.*, 2024] Yazhou Ren, Jingyu Pu, Zhimeng Yang, Jie Xu, Guofeng Li, Xiaorong Pu, Philip S. Yu, and Lifang He. Deep clustering: A comprehensive survey. *IEEE Transactions on Neural Networks and Learning Systems*, 2024.
- [Ronneberger *et al.*, 2015] Olaf Ronneberger, Philipp Fischer, and Thomas Brox. U-net: Convolutional networks for biomedical image segmentation. In *Medical Image Computing and Computer-Assisted Intervention (MICCAI)*, 2015.
- [Saharia *et al.*, 2021] Chitwan Saharia, Jonathan Ho, William Chan, Tim Salimans, David J. Fleet, and Mohammad Norouzi. Image super-resolution via iterative refinement, 2021.
- [Saharia *et al.*, 2022] Chitwan Saharia, William Chan, Saurabh Saxena, Lala Li, Jay Whang, Emily L. Denton, Seyed Kamyar Seyed Ghasemipour, Raphael Gontijo Lopes, Burcu Karagol Ayan, Tim Salimans, Jonathan Ho, David J. Fleet, and Mohammad Norouzi. Photorealistic text-to-image diffusion models with deep language understanding. In *Advances in Neural Information Processing Systems 35 (NeurIPS 2022)*, 2022.
- [Song and Ermon, 2021] Yang Song and Stefano Ermon. Score-based generative modeling through stochastic dif-

- ferential equations. In *International Conference on Learning Representations (ICLR)*, 2021.
- [Tang *et al.*, 2023] Luming Tang, Menglin Jia, Qianqian Wang, Cheng Perng Phoo, and Bharath Hariharan. Emergent correspondence from image diffusion. In *Advances in Neural Information Processing Systems*, volume 36, 2023.
- [Uziel *et al.*, 2025] Roy Uziel, Irit Chelly, Oren Freifeld, and Ari Pakman. Clustering via self-supervised diffusion. In *Proceedings of the 42nd International Conference on Machine Learning*, volume 267 of *Proceedings of Machine Learning Research*, pages 60711–60726. PMLR, 13–19 Jul 2025.
- [Van Gansbeke *et al.*, 2020] Wouter Van Gansbeke, Simon Vandenhende, Stamatios Georgoulis, Marc Proesmans, and Luc Van Gool. Scan: Learning to classify images without labels. In *Computer Vision – ECCV 2020*, pages 268–285. Springer, 2020.
- [Wang *et al.*, 2023] Yingheng Wang, Yair Schiff, Aaron Gokaslan, Weishen Pan, Fei Wang, Christopher De Sa, and Volodymyr Kuleshov. Infodiffusion: Representation learning using information maximizing diffusion models. In *Proceedings of the 40th International Conference on Machine Learning (ICML)*, volume 202 of *Proceedings of Machine Learning Research*, pages 36336–36354, 2023.
- [Wei *et al.*, 2024] Xiuxi Wei, Zhihui Zhang, Huajuan Huang, and Yongquan Zhou. An overview on deep clustering. *Neurocomputing*, 590:127761, 2024.
- [Xiang *et al.*, 2023] Weilai Xiang, Hongyu Yang, Di Huang, and Yunhong Wang. Denoising diffusion autoencoders are unified self-supervised learners. In *Proceedings of the IEEE/CVF International Conference on Computer Vision (ICCV)*, pages 15802–15812, October 2023.
- [Xie *et al.*, 2016] Junyuan Xie, Ross B. Girshick, and Ali Farhadi. Unsupervised deep embedding for clustering analysis. In *Proceedings of the 33rd International Conference on Machine Learning (ICML)*, volume 48 of *JMLR Workshop and Conference Proceedings*, pages 478–487, 2016.
- [Yan *et al.*, 2025] Jie Yan, Jing Liu, and Zhong-Yuan Zhang. Clusterddpm: An em clustering framework with denoising diffusion probabilistic models. *Information Sciences*, 720:122518, December 2025.
- [Zhou *et al.*, 2024a] Sheng Zhou, Hongjia Xu, Zhuonan Zheng, Jiawei Chen, Zhao Li, Jiajun Bu, Jia Wu, Xin Wang, Wenwu Zhu, and Martin Ester. A comprehensive survey on deep clustering: Taxonomy, challenges, and future directions. *ACM Computing Surveys*, 2024.
- [Zhou *et al.*, 2024b] Sheng Zhou, Hongjia Xu, Zhuonan Zheng, Jiawei Chen, Zhao Li, Jiajun Bu, Jia Wu, Xin Wang, Wenwu Zhu, and Martin Ester. A comprehensive survey on deep clustering: Taxonomy, challenges, and future directions. *ACM Computing Surveys*, 57(3):1–38, 2024.